

# Evidence for an Excited-State Reaction Contributing to NADH Fluorescence

Alexey S. Ladokhin<sup>1,2,3</sup> and Ludwig Brand<sup>1</sup>

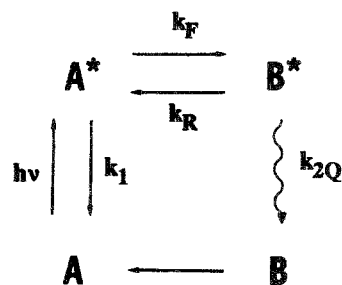
Received March 8, 1994; revised June 24, 1994; accepted June 27, 1994

The fluorescence of reduced  $\beta$ -nicotinamide adenine dinucleotide (NADH) was monitored as a function of the excitation and emission wavelengths. In aqueous and organic solvents the intensity decay was found to be more heterogeneous than reported earlier. When the ternary complex of NADH with the enzyme (horse liver alcohol dehydrogenase) and substrate analog (iso-butyramide) is formed, three exponents are required to fit the data. The decay-associated spectrum for the shortest lifetime undergoes a sign change from positive at the blue edge of emission to negative at the red edge. This phenomenon is interpreted as an outcome of reversible excited-state reaction leading to the appearance of at least one fluorescent product.

**KEY WORDS:** NADH; decay-associated spectra; excited-state reaction.

## INTRODUCTION

The fluorescence properties of NADH (reduced  $\beta$ -nicotinamide adenine dinucleotide) have been a subject of multiple studies [1–4]. In aqueous solution the quantum yield of fluorescence is low and the average lifetime is in the subnanosecond range. In organic solvents the lifetime increases while spectral position undergoes a blue shift. Binding to LADH (horse liver alcohol dehydrogenase, E.C. 1.1.1.1) leads to a further blue shift in absorbance and fluorescence and a dramatic increase in both lifetime and quantum yield. This effect is enhanced by formation of a ternary complex with the substrate analog iso-butyramide (IBA). For more details and references see review by Ross *et al.* [5].



## NADH

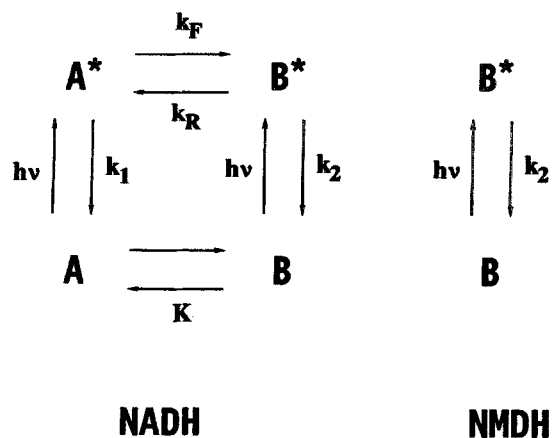
Scheme 1.

<sup>1</sup> McCollum-Pratt Institute, Department of Biology, Johns Hopkins University, Baltimore, Maryland 21218.

<sup>2</sup> Permanent address: Palladin Institute of Biochemistry, Ukrainian Academy of Sciences, Kiev 252030, Ukraine.

<sup>3</sup> To whom correspondence should be addressed. Current address: Department of Physiology and Biophysics, University of California-Irvine College of Medicine, Irvine, California 92717.

Despite the fact that the fluorescence properties of reduced nicotinamide nucleotides have been extensively studied, there is no consensus either on the degree of deviation from monoexponentiality [6] or on possible origins of lifetime heterogeneity. Proposed mechanisms include the presence of different emitting species [3],



Scheme 2.

reversible excited-state reaction forming a nonfluorescent product [2], and exciplex formation [4].

Two different models suggested in the literature are presented in Schemes 1 and 2. The earlier proposed model [2] is depicted in Scheme 1. It describes a reversible excited-state reaction with nonfluorescent product ( $B^*$ ) and no heterogeneity in the ground state of reduced nicotinamide (A). Here  $k_{2Q}$  is a nonradiative rate, while  $k_1$  is the sum of radiative and nonradiative rates. This model predicts that the fluorescence decay will be double exponential and will not depend on emission wavelength. Both those facts were reported to be confirmed experimentally [2].

The second model (Scheme 2) was proposed to explain the kinetic fluorescence of both mononucleotides (NMNH) and dinucleotides (NADH) [4]. It assumes that the stacked conformation of NADH (A,  $A^*$ ) is in equilibrium with the open one (B,  $B^*$ ) in both ground and excited states. The open conformation is believed to have the same fluorescence properties as NMNH. In the limiting case of very slow folding the fluorescence decay is predicted to follow a biexponential law. The two lifetimes would represent decays of pure stacked and open conformations and the preexponential factors would be connected to the A and B concentrations at equilibrium. This model was supported by the fact that decay of NMNH is virtually monoexponential and that its lifetime is similar to the short component of the NADH decay [4].

In this study fluorescence of NADH in different solvents and when bound to LADH was studied as a function of the excitation and emission wavelengths by means of steady-state, frequency-domain, and photon counting pulse fluorometry. Results are used to reconsider existing models explaining fluorescence of pyridine

nucleotide coenzymes. A preliminary account of this work has appeared elsewhere [7].

## MATERIALS AND METHODS

Reduced  $\beta$ -NADH was obtained from Sigma (St. Louis, MO) and iso-butyramide from Aldrich Chemical Co (Milwaukee, WI). Organic solvents were methanol, spectrophotometric grade, from Aldrich Chemical Co (Milwaukee, WI), ethanol, anhydrous, from Warner-Graham Co (Cockeysville, MD), and glycerol, glass distilled, from EM Science (Gibbstown, NJ). Liver alcohol dehydrogenase was obtained from Boehringer Mannheim (Germany) as a crystalline suspension, which was dialyzed against several fresh additions of 0.1 M sodium phosphate buffer pH 7 (this buffer was used through all the measurements and will be referred as "buffer" or "aqueous buffer"). The final concentration was determined spectrophotometrically using an extinction coefficient of  $35.3 \text{ mM}^{-1} \text{ cm}^{-1}$  at 280 nm for LADH and  $6.18 \text{ mM}^{-1} \text{ cm}^{-1}$  at 334 nm for NADH in buffer [5]. The binary complex (NADH-LADH) was prepared by adding a proper amount of LADH to NADH until the final concentrations ( $14 \text{ }\mu\text{M}$  NADH,  $57 \text{ }\mu\text{M}$  LADH) were reached. The ternary complex was prepared by adding stock solution of iso-butyramide (IBA) to the final concentration of 10 mM. Concentrations of NADH and LADH in ternary complex were 13 and  $39 \text{ }\mu\text{M}$ , respectively. Under these conditions, according to the data available in the literature [8,9], virtually all the NADH was bound in a ternary complex, and for the binary complex the percentage of unbound NADH did not exceed 5%.

Absorbance was measured on the single-beam spectrophotometer LKB 4050 (LKB Biochrom, Cambridge, England). To avoid inner filter effects, samples with an optical density less than 0.1 were used for fluorescence studies. Steady-state and frequency-domain measurements were carried out on the SLM-48000 multifrequency phase-and-modulation spectrofluorometer (SLM Instruments Inc., Urbana, IL). For the steady-state measurements a Xe arc lamp was used. Excitation and emission wavelengths were selected by a single-grating monochromators with 4-nm slits. To improve accuracy in determining the spectral position the following procedure was utilized: emission spectra were recorded from 350 to 650 nm with a 1-nm increment and after background correction were fitted to a log-normal distribution [10] to yield position of maximal intensity. In frequency-domain measurements, either the 325-nm line of a He-Cd laser or the 365-nm Hg line was used for

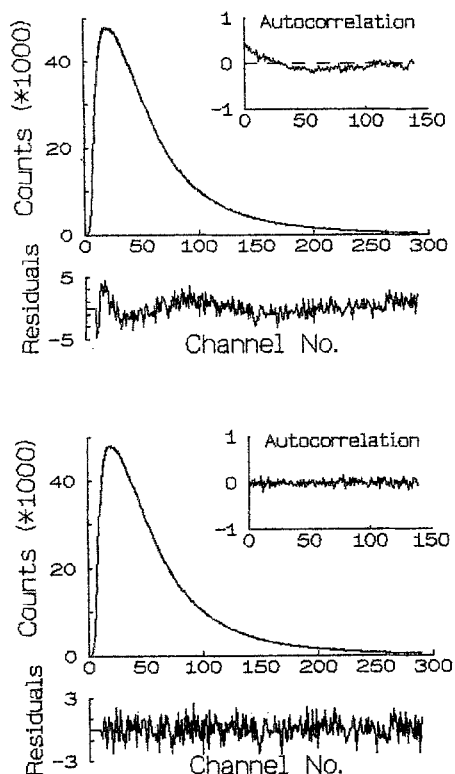


**Fig. 1A.** Experimental decay curves and the results of an analysis with different numbers of exponents for the NADH in aqueous buffer at +14°C. The excitation wavelength was 330 nm and the emission registration wavelength was 460 nm. The timing calibration was 11 ps/channel. Parameters recovered by best double-exponential fit (upper panel) are:  $\alpha_1 = 59\%$ ,  $\tau_1 = 0.26$  ns;  $\alpha_2 = 41\%$ ,  $\tau_2 = 0.63$  ns; reduced  $\chi^2 = 1.88$ . Parameters recovered by best triple-exponential fit (lower panel) are:  $\alpha_1 = 21\%$ ,  $\tau_1 = 0.12$  ns;  $\alpha_2 = 60\%$ ,  $\tau_2 = 0.37$  ns;  $\alpha_3 = 19\%$ ,  $\tau_3 = 0.76$  ns; reduced  $\chi^2 = 1.11$ .

excitation. In the latter case the light from a 200-W Hg-Xe arc lamp (Spectral Energy Corp., Westwood, NJ) was passed through a combination of Corning 7-60 and 0-52 filters. Emission light was monitored through the short-cutoff KV-399 filter. For data analysis, errors were individually calculated based on ten repeated measurements at each frequency. To avoid systematic errors associated with the color effect [11], a fluorescence single lifetime reference was employed (POPOP in ethanol,  $\tau = 1.29$  ns).

Time-resolved fluorescence decays were collected with a time-correlated single photon counting apparatus as described earlier [12]. The cavity-dumped output of a synchronously pumped rhodamine-6G or DCM dye laser was used to generate a laser pulse, which was then frequency-doubled to 297 or 330 nm, respectively. Emission was spectrally selected with monochromator

with 8-nm spectral resolution and detected with the microchannel plate.

For all types of fluorescence measurements a magic angle configuration of polarizers was used to exclude the artifacts associated with dynamic depolarization [13].

Both simulated and experimental data were analyzed by the nonlinear least-squares method assuming that fluorescence decay can be represented as a sum of exponential components:  $I(t) = \sum \alpha_i \exp(-t/\tau_i)$ . Scattering from the Ludox solution was used as a reference with a zero lifetime. To recover decay-associated spectra (DAS), a series of kinetics measured at different wavelength were analyzed globally by linking the lifetime and allowing  $\alpha$ 's to float independently. The preexponential factors were normalized to yield intensity, calculated as  $\sum \alpha_i \tau_i$ , to be proportional to the steady-state intensity measured independently. The DAS for binary and ternary NADH complexes at different temperatures were normalized together to produce the same intensity ratio as their steady-state spectra. The steady-state spectrum of ternary complex at 6°C was normalized to 100. For the presentation in tables the preexponential terms were normalized to a sum of 100%.

## RESULTS

### Fluorescence of NADH in Aqueous and Organic Solvents

The fluorescence decay data on NADH in buffer measured by the pulse technique are presented in Fig. 1A. The best double-exponential fit is shown in the upper panel, and as revealed by autocorrelation and distribution of residuals, it has nonrandom deviations from experimental data. A three-component analysis (lower panel) is free of those deviations and yields lower  $\chi^2$  (Tables I and II). However, obtained lifetimes seemed to be rather narrowly spaced to prove that three distinct components are indeed observed. To check on our ability to recover such lifetimes, a number of simulations were performed. Figure 1B shows the best two- and three-exponential fits to the simulated data obtained by convolving the same lamp profile with the three-exponential decay. The Poisson noise and a small component with the zero lifetime were added to the decay curve to get a more realistic situation. As one can see from the autocorrelation, distribution of residues, and  $\chi^2$ , the three-exponential fit is more adequate and recovered parameters coincide with those input. However, the reduced  $\chi^2$  for the simulated data is lower than that for the experimental results. It is difficult to say whether this is

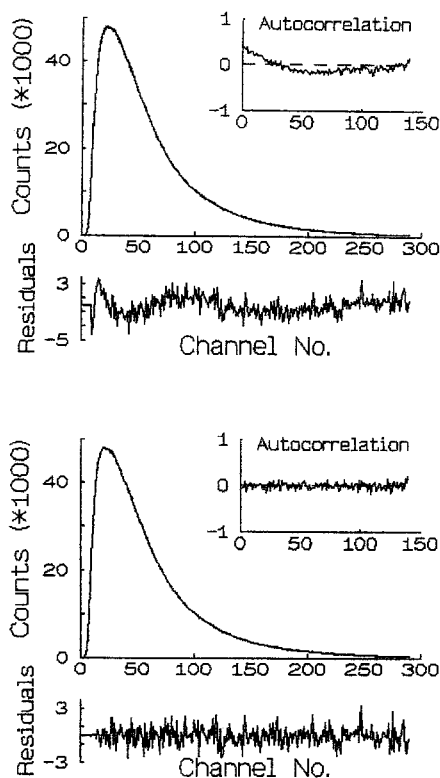


**Fig. 1B.** Simulated decay curves and the results of an analysis with different numbers of exponents. Parameters for the triple-exponential fit from the legend for Fig. 1A were used to generate decay (see text for details). Parameters recovered by best double-exponential fit (upper panel) are:  $\alpha_1 = 66\%$ ,  $\tau_1 = 0.29$  ns;  $\alpha_2 = 34\%$ ,  $\tau_2 = 0.67$  ns; reduced  $\chi^2 = 1.80$ . Parameters recovered by best triple-exponential fit (lower panel) are:  $\alpha_1 = 20\%$ ,  $\tau_1 = 0.12$  ns;  $\alpha_2 = 60\%$ ,  $\tau_2 = 0.36$  ns;  $\alpha_3 = 20\%$ ,  $\tau_3 = 0.75$  ns; reduced  $\chi^2 = 1.06$ .

due to the possible contribution of nonrandom errors or whether real decay follows an even more complex law.

The heterogeneity of decay becomes even more pronounced when organic solvents are used (Table I). Double-exponential analysis was not adequate to fit the data. On the other hand, addition of a fourth component leads to only marginal improvements of the fit in most cases and always yields practically the same average lifetime as the three-component analysis. The spectral dependences of the amplitude average lifetime ( $\tau_\alpha = \sum \alpha_i \tau_i / \sum \alpha_i$ ) for NADH in methanol are presented in Fig. 2 and show an increase with increase of excitation and emission wavelength. This was found to be true for all the solvents (data not shown).

To further address the question of the excitation dependence of NADH, fluorescence phase/modulation and steady-state spectroscopy were applied. It should be pointed out that the phase instrument allows the excitation source to be easily changed to the same sample

can readily be measured at two excitation wavelengths. Table II summarizes the results for the temperature dependence of NADH fluorescence decay in aqueous buffer. In all the cases, due to lower resolution of the SLM-48000 phase instrument as compared to the pulse instrument used, only two components were recovered. At all temperatures the average lifetime measured at 325-nm excitation is shorter than that with 365-nm excitation. (The same was true for a triple-exponential analysis despite the fact that solutions in this case were not unique and depended on the initial guess.) However, the preexponential factor for the short lifetime follows the opposite pattern, and increase in  $\tau_\alpha$  is solely due to an increase in both lifetimes. This implies that a simple explanation for the excitation dependence involving two distinct noninteracting species with different lifetimes and different excitation spectra is not applicable.

The slight but detectable dependence of steady-state spectra on excitation was also found for NADH in all solvents (Fig. 3). In the glycerol solution this dependence is quite strong at the red edge of absorption, as is expected for photoselection in a system with slow (comparable to a lifetime) dipole relaxation [14]. For all the other solvents, orientational relaxation is much too fast to contribute to the spectral shift (see also Discussion).

### Fluorescence of the Protein-Bound NADH

Fluorescence decay parameters of NADH bound to LADH with or without IBA are presented in Table III. To ensure that no heterogeneity in fluorescence is caused by the existence of two binding sites on the LADH molecule, an excess of protein (3 mol LADH per 1 mol NADH) was used.

The formation of a binary complex (NADH-LADH) results in 4.5-fold increase of average lifetime, which is in agreement with the earlier report, where biexponential fluorescence decay was used [2]. In contrast, in the present study we found that a much more complex decay law is needed to describe the system. A minimum of three exponents was required, and at the blue wing of emission (420 nm in Table III) a fourth component brought further improvement to the fit. In order to improve spectral resolution of components, a linked (global) analysis of decay data measured at a different wavelength was performed. For this procedure the lifetimes were linked together across the emission spectrum, while preexponential factors were allowed to float independently. Introduction of the fourth component appears to be important for the global analysis. The global reduced  $\chi^2$  of 1.7 was achieved with three components and 1.17 with four components. In order to recover de-

**Table I.** Best Fit Parameters of Fluorescence Decay of NADH in Different Solvents<sup>a</sup>

Solvent	$\alpha_1$ (%), $\tau_1$ (ns)	$\alpha_2$ (%), $\tau_2$ (ns)	$\alpha_3$ (%), $\tau_3$ (ns)	$\alpha_4$ (%), $\tau_4$ (ns)	$\chi^2$	$\tau_o$ (ns)
Aqueous buffer	67, 0.23	33, 0.56			1.52	0.34
	38, 0.18	47, 0.37	15, 0.65		1.22	0.34
Methanol	76, 0.37	24, 1.18			9.2	0.56
	38, 0.18	55, 0.58	7, 1.77		1.23	0.51
	21, 0.10	37, 0.32	37, 0.71	4, 2.1	1.05	0.50
Ethanol	85, 0.47	15, 1.72			10.4	0.66
	40, 0.20	54, 0.68	6, 2.41		1.22	0.58
	23, 0.11	38, 0.37	36, 0.84	3, 2.9	1.02	0.56

<sup>a</sup>Measurements were carried out at 24°C with the photon counting pulse technique under 330-nm excitation and 440-nm emission.

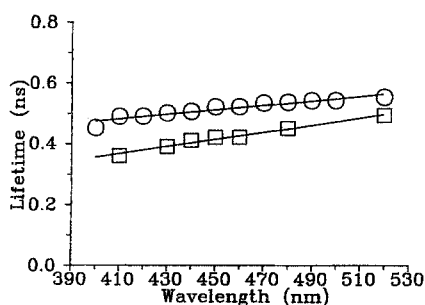


**Fig. 2.** Average lifetime of NADH in methanol measured as a function of emission wavelength with excitation at 297 nm ( $\square$ ) and 330 nm ( $\circ$ ).

**Table II.** Best Fit Parameters of the Fluorescence Decay of NADH in Aqueous Buffer Measured by Fluorescence Phase/Modulation Spectroscopy<sup>a</sup>

$t$ (°C)	Excitation 325 nm	Excitation 365 nm
+8	$\tau_1 = 0.37$ ns; $\alpha_1 = 81\%$ $\tau_2 = 0.96$ ns; $\alpha_2 = 19\%$ $\tau_o = 0.48$ ns	$\tau_1 = 0.44$ ns; $\alpha_1 = 83\%$ $\tau_2 = 1.07$ ns; $\alpha_2 = 17\%$ $\tau_o = 0.55$ ns
+24	$\tau_1 = 0.25$ ns; $\alpha_1 = 80\%$ $\tau_2 = 0.72$ ns; $\alpha_2 = 20\%$ $\tau_o = 0.34$ ns	$\tau_1 = 0.33$ ns; $\alpha_1 = 85\%$ $\tau_2 = 0.84$ ns; $\alpha_2 = 15\%$ $\tau_o = 0.41$ ns
+35	$\tau_1 = 0.12$ ns; $\alpha_1 = 81\%$ $\tau_2 = 0.58$ ns; $\alpha_2 = 19\%$ $\tau_o = 0.21$ ns	$\tau_1 = 0.29$ ns; $\alpha_1 = 90\%$ $\tau_2 = 0.82$ ns; $\alpha_2 = 10\%$ $\tau_o = 0.34$ ns

<sup>a</sup>The reduced  $\chi^2$  was in the range of 1.05–1.26.

cay-associated spectra (DAS) for individual lifetimes the  $\alpha$ 's were normalized to produce the steady-state spectrum measured independently (see Methods for details). The DAS for the NADH–LADH binary complex are presented in Fig. 4. A slight spectral difference leads to a greater contribution of longer-lived components at greater wavelength.

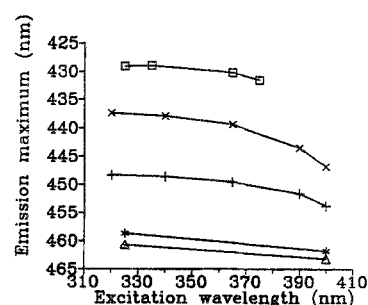


**Fig. 3.** Dependence of the steady-state fluorescence spectra on the excitation wavelength for NADH in (from top to bottom) ternary complex (NADH–LADH–IBA) at +8°C, glycerol at +12°C and at +50°C, and aqueous buffer at +8°C and at +24°C.

When the ternary complex is formed (NADH–LADH–IBA) the fluorescence decay simplifies somewhat (Table III). Four components are no longer needed, and in a particular wavelength region (approximately at the emission maximum) decay is adequately described by two exponents. However, a peculiar feature appears: a component with a *negative* amplitude is essentially important to get an acceptable fit when fluorescence is measured at the red edge of emission. On the far blue edge a component with a similar lifetime has a positive amplitude. Two longer lifetimes appear to be very similar across the spectrum. This provides a rationale for using the global analysis with the linked lifetimes. The DAS for NADH–LADH–IBA ternary complex obtained by this procedure are shown in Figs. 5A (14°C) and 5B (6°C). They appear to be very similar for both temperatures. The longest component dominates and it is responsible for the greatest portion of steady-state intensity (up to 80%). This is the only component with a temperature-dependent lifetime. An intermediate component has slightly-blue shifted spectrum, while the shortest undergoes a sign change and becomes negative at the

**Table III.** Best Fit Parameters of Fluorescence Decay of NADH in Different Complexes with LADH<sup>a</sup>

Complex	$\alpha_1$ (%), $\tau_1$ (ns)	$\alpha_2$ (%), $\tau_2$ (ns)	$\alpha_3$ (%), $\tau_3$ (ns)	$\alpha_4$ (%), $\tau_4$ (ns)	$\chi^2$	$\tau_a$ (ns)
Free NADH 460 nm	59, 0.26	41, 0.63			1.88	0.41
	21, 0.12	60, 0.37	19, 0.76		1.11	0.39
Binary complex 420 nm	47, 0.90	53, 3.14			4.3	2.08
	26, 0.29	45, 1.68	29, 3.66		1.22	1.89
	18, 0.13	22, 0.68	50, 2.3	10, 4.8	1.06	1.80
Binary complex 460 nm	42, 0.98	58, 3.07			3.8	2.19
	21, 0.38	47, 1.82	32, 3.58		1.07	2.07
Ternary complex 420 nm	20, 1.47	80, 5.47			1.64	4.69
	13, 0.19	18, 2.23	69, 5.58		1.02	4.30
Ternary complex 460 nm	21, 2.64	79, 5.63			1.06	5.01
	-10, 0.06	21, 2.46	89, 5.59		1.02	5.47
Ternary complex 500 nm	32, 3.59	68, 5.84			1.92	5.12
	-26, 0.10	22, 2.54	104, 5.58		1.09	6.32

<sup>a</sup>Measurements were carried out at 14°C with photon counting pulse technique under 330-nm excitation.

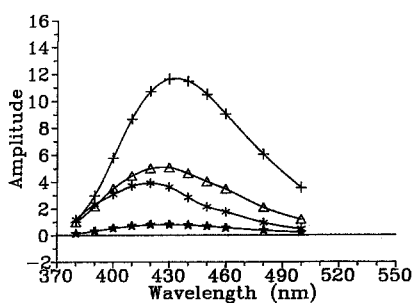


**Fig. 4.** DAS of binary complex (NADH-LADH) measured with 330-nm excitation at 14°C. Spectra correspond to the following lifetimes: 0.15 ns (\*); 0.80 ns ( $\Delta$ ); 2.56 ns (+); 6.41 ns ( $\star$ ). Global reduced  $\chi^2 = 1.17$ .

wavelength  $>440$  nm. This behavior indicates the existence of an excited-state reaction [15].

## DISCUSSION

Earlier results obtained with binary (NADH-LADH) and ternary (NADH-LADH-IBA) complexes were shown to be in a good agreement with a double-exponential decay [2]. However, the time resolution of those studies was limited by the use of a flash lamp. Improvement of the pulse technique allows us to recover and analyze more than two components. Application of global analysis [16] of the data collected at different wavelengths provides the possibility of improving spectral resolution and interpreting our results in terms of decay-associated spectra (DAS).

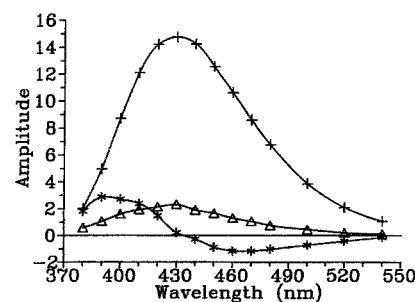
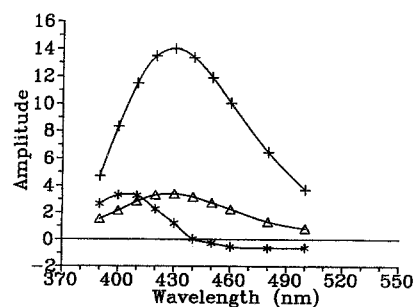


**Fig. 5.** DAS of ternary complex (NADH-LADH-IBA) measured with 330-nm excitation at (A) 14°C, and (B) 6°C. Spectra correspond to the following lifetimes: (A) 0.22 ns (\*); 2.17 ns ( $\Delta$ ); 5.56 ns (+). Global reduced  $\chi^2 = 1.10$ . (B) 0.26 ns (\*); 2.13 ns ( $\Delta$ ); 6.41 ns (+). Global reduced  $\chi^2 = 1.19$ .

Combination of these two conditions (advanced pulse technology and a global analysis) allowed us to provide evidence that the excited-state reaction contributes to the NADH fluorescence. This evidence comes from the existence of a negative component in the DAS of the ternary complex (Fig. 5). Moreover it implies that unlike earlier suggestions (Scheme 1), the “product” of

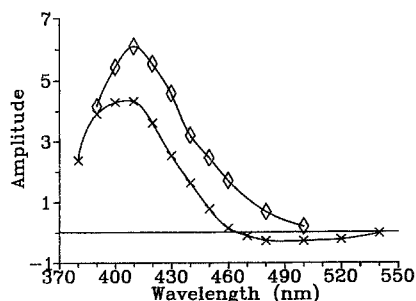


Fig. 6. Sum of the DAS of the two shortest components from Fig. 5 for ( $\diamond$ ) 14°C and ( $\times$ ) 6°C.

the excited-state reaction is fluorescent. Similar DAS were reported for excited-state proton transfer in aromatic alcohols [15]. Later studies contain several important conclusions based on experimental observation and simulations of two-state excited-state reactions with no heterogeneity in the ground state:

(i) Negative amplitudes are always associated with the shortest lifetime.

(ii) The DAS “involved” in an excited-state reaction have mirror symmetry at the longer wavelength.

(iii) Existence of a region of positive amplitude (usually blue edge of emission) for a component with negative amplitude in another region (usually red edge) indicates the reversibility of the excited-state reaction, and that depletion from the directly excited state (“substrate”) occurs faster than that from the state populated by the reaction (“product”).

All of the aforementioned are characteristic for NADH fluorescence in ternary complex. However, other evidence might significantly complicate direct applicability of these conclusions to our case.

First of all, we observe three decay components, not two, predicted for two-state reactions [17,18] and observed for aromatic alcohols [15]. It is possible that only two components are involved in the reaction and that the third (with the longest lifetime) originates from an independently excited and depleted state. In this case we will still have a two-state reaction. As it was predicted earlier [18] for such reactions (with no heterogeneity in the ground state), the sum of the DAS represents a species-associated spectrum (SAS) of the “product” and thus should always be positive. The results of such summation of DAS corresponding to the shortest and intermediate decay times for NADH in ternary complex are presented in Fig. 6. It is rather difficult to conclude whether a negative component observed at 6°C is real or is due to experimental error. The shape of

the curves is also somewhat different for the two temperatures, which could hardly be explained if only two states are involved in the reaction.

Second, it seems to be rather difficult to prove (or disprove) that no heterogeneity exists in the ground state and that no direct excitation of “product” occurs. One of the possibilities to do so is to analyze the excitation dependence of fluorescence. Unfortunately, one can hardly expect dramatic changes in fluorescence of the ternary complex with the change of excitation, since a long-lived component (whose participation in the reaction is questionable) dominates the decay and steady-state spectra. Only a marginal spectral shift with excitation is observed (curve 1 on Fig. 3). Indirect evidence on this matter might come from fluorescence properties of NADH in solution.

It appears that both temporal and energetic properties of NADH fluorescence in solution depend on excitation wavelength (Table II, Figs. 2 and 3). One possible explanation of a spectral shift in emission seen with the change in excitation wavelength is a photoselection of chromophores with different energies of interaction with the solvent shell [14]. Two requirements to observe such effects are the existence of the distribution of energies of interaction within the solvate and *slow* relaxation which will not allow photoselected states to be “remixed” prior to emission. This, however, cannot explain the spectral shift observed with NADH in buffer when the excitation or temperature is changed, since relaxation of water dipoles occurs on a subpicosecond time scale. Moreover, existence of “red-edge effects” at 50°C in glycerol is quite unusual and was not observed for fluorescence of indole or tryptophan [14]. In the latter case, but at lower temperatures, the position of the emission spectrum was invariant with the excitation wavelength in the mean band absorbance until the “red edge” ( $\lambda > 290$  nm for tryptophan) is reached. This is clearly not the case with NADH in glycerol solution (Fig. 3), whose curves will not flatten even at the blue edge of absorbance. This is a minor effect and the main contribution to the excitation-dependent spectral shift for NADH in *glycerol* comes from photoselection of chromophores with different energies of dipole interaction within a solvate. Certainly, some other kind of ground-state heterogeneity should be involved in the explanation of the excitation dependence of NADH in *nonviscous* solvents. Visser and van Hoek [4] reported a small spectral shift between the fluorescence of NADH and NMNH (reduced  $\beta$ -nicotinamide mononucleotide) which they initially attributed to an exciplex formation in dinucleotide. It seems reasonable to suggest that stacking of NADH suggested in Scheme 2 will produce

two ground-state forms A and B with somewhat different spectral properties. This can occur either via direct interaction of rings or indirectly by providing shielding from the influence of the solvent.

The "stacking model" presented in Scheme 2 was also used to explain a biexponential decay of NADH in aqueous buffer [4]. Our results suggest that the fluorescence decay is more complex and does not follow a biexponential law (Table I). A few empirical observations can be emphasized from these data. With the decrease of polarity (i) the average lifetime increases, (ii) the ratio of longest to shortest lifetime increases, and (iii) heterogeneity of decay increases. It is also peculiar that an uncertain but high number of exponents (three or four) is required to describe decay with such a short average lifetime. This behavior is more reminiscent of a continuous distribution of decay times rather a discrete number of exponents.

## CONCLUSIONS

Our findings suggest that the excited-state reaction that governs NADH fluorescence is reversible and yields a *fluorescent* product. In solution, the *ground-state heterogeneity* is apparent and at least two forms with different excitation and emission spectra coexist in equilibrium. The interconversion between those forms occurs on the same time scale as the depletion of excited states. It is possible that in all systems, with the exception of a ternary complex, a *distribution of reaction rates* exists. This leads to an infinite number of lifetimes. The distribution of the reaction rates depends on the polarity of the solvent. In the case of the binary complex, the protein serves as a matrix to keep NADH at low polarity where it otherwise would not be soluble. Addition of a substrate (or an analog in ternary complex) provides a condition where a broad distribution of decay rates of the excited-state reaction reduces to a *finite* (if not unique) number of rates.

The conclusions of the study presented here certainly are mainly empirical. Much work needs to be done to answer some specific questions. Is this a two- or higher state reaction? Is there a direct excitation of "product" species in the ternary complex, or is the slight observed dependence on excitation wavelength

due to a photoselection of a subpopulation of molecules that have an electronic configuration close to one of the "products," as was suggested for intramolecular electron transfer in bianthryl [19]. Perhaps the answers will bring us closer to an understanding of what the mechanism of the reaction is and how relevant it is to the biological function of NADH.

## ACKNOWLEDGMENTS

This work was supported by NIH grant GM11632, NSF Biological Research Centers Award DIR-8721059, and a W. M. Keck Foundation Award. The authors are grateful to Drs. K. M. Hirshfield, D. Toptygin, and P. Wu for their technical assistance. The authors would like to acknowledge Drs. J. M. Beechem, L. Davenport, A. Gafni, J. R. Knutson, and A. J. W. G. Visser for helpful discussions.

## REFERENCES

1. T. G. Scott, R. D. Spencer, N. J. Leonard, and G. Weber (1970) *J. Am. Chem. Soc.* **92**, 687–695.
2. A. Gafni and L. Brand (1976) *Biochemistry* **15**, 3165–3171.
3. J. C. Brochon, Ph. Wahl, J.-M. Jallon, and M. Iwatsubo (1976) *Biochemistry* **15**, 3259–3265.
4. A. J. W. G. Visser and A. van Hoek (1981) *Photochem. Photobiol.* **33**, 35–40.
5. J. B. A. Ross, S. Subramanian, and L. Brand (1982) in J. Everse, B. Anderson, and K.-S. You (Eds.), *The Pyridine Nucleotide Coenzymes*, Academic Press, New York, pp. 19–49.
6. M. R. Eftink (1992), *Adv. Biophys. Chem.* **2**, 81–114.
7. A. S. Ladokhin and L. Brand (1993) *Biophys. J.* **64**, A53.
8. H. Theorell and A. D. Winer (1959) *Arch. Biochem. Biophys.* **83**, 291–293.
9. T. Yonehtani and H. Theorell (1962) *Arch. Biochem. Biophys.* **99**, 433–437.
10. A. S. Ladokhin, L. Wang, A. W. Steggle, and P. W. Holloway (1991) *Biochemistry* **30**, 10200–10206.
11. J. R. Lakowicz, H. Cherek, and A. Balter (1981) *J. Biochem. Biophys. Meth.* **5**, 131.
12. M. Badea and L. Brand (1979) *Meth. Enzymol.* **61**, 378–425.
13. M. Shinitzky (1972) *J. Chem. Phys.* **56**, 5979.
14. A. P. Demchenko and A. S. Ladokhin (1988) *Eur. Biophys. J.* **15**, 369–379.
15. L. Davenport, J. R. Knutson, and L. Brand (1986) *Biochemistry* **25**, 1186–1195.
16. J. M. Beechem, M. Ameloot, and L. Brand (1985) *Chem. Phys. Lett.* **120**, 466–472.
17. J. B. Birks (1970), *Photophysics of Aromatic Molecules*, Wiley, New York.
18. W. R. Laws and L. Brand (1979) *J. Phys. Chem.* **83**, 795–802.
19. A. P. Demchenko, and A. I. Sytnik (1991) *Proc. Natl. Acad. Sci. USA* **88**, 9311–9314.